Dynamic depletion attraction between colloids suspended in a phase-separating binary liquid mixture

2008 J. Phys.: Condens. Matter 20 072101

(http://iopscience.iop.org/0953-8984/20/7/072101)

IOP FTC
IOP PUBLISHING JOURNAL OF PHYSICS: CONDENSED MATTER
J. Phys.: Condens. Matter **20** (2008) 072101 (6pp) doi:10.1088/0953-8984/20/7/072101

FAST TRACK COMMUNICATION

Dynamic depletion attraction between colloids suspended in a phase-separating binary liquid mixture

Takeaki Araki and Hajime Tanaka

Institute of Industrial Science, University of Tokyo, Meguro-ku, Tokyo 153-8505, Japan

E-mail: takeaki@iis.u-tokyo.ac.jp and tanaka@iis.u-tokyo.ac.jp

Received 12 December 2007
Published 31 January 2008
Online at stacks.iop.org/JPhysCM/20/072101

Abstract

Understanding interactions between colloids (or nanoparticles) immersed in a phase-separating binary mixture is of both fundamental and technological importance. Here we report a novel type of interparticle attractive interaction of a purely dynamic origin, which is found by a coarse-grained numerical simulation. Due to surface wetting effects, there are strong diffusion fluxes towards particles just after the initiation of phase separation of the matrix binary liquid mixture. The flux in the region between particles soon becomes weaker than that in the other regions since the depletion zones formed around particles overlap selectively between the particles. The resulting imbalance of the diffusion flux induces interparticle attractive interactions, i.e., the osmotic force pushes particles closer. We confirm that this wetting-induced 'dynamic' depletion force can be stronger than a van der Waals force and a capillary force that is induced by the interfacial tension, and thus plays a dominant role in the early stage of particle aggregation. We note that this novel interaction originating from the momentum conservation law may be generic to particles acting as diffusional sinks or sources.

(Some figures in this article are in colour only in the electronic version)

Suspensions of colloids or nanoparticles in complex fluids, such as liquid crystals [1] and polymer solutions [2], have attracted considerable attention from the fundamental and practical importance viewpoints. Colloidal suspensions in a binary mixture of simple liquids also exhibit quite rich behaviour [3]. For example, when colloids are suspended in a near critical binary mixture above the critical temperature T_c, preferential wetting of one of the components [4, 5] on colloid surfaces leads to colloid aggregation or flocculation [6, 7]. The underlying mechanism has been intensively studied theoretically [7–13]. The confinement effect on the compositional fluctuations also generates an interaction between particle surfaces. This force between particles, whose strength and direction depend upon the wettability of the particles, is known as a critical Casimir force [13, 14].

It is widely known that below T_c wetting phenomena drastically affect phase separation and the resulting pattern evolution [15, 16]. Addition of particles into a binary liquid mixture induces complex dynamic couplings between wetting and phase separation due to the mobility of particles and produces a rich variety of morphologies [16–27]. When a particle equally wets the two phase-separated phases, then such neutral particles can sit just on the domain interface, leading to Pickering emulsions [28] or noble glassy bicontinuous structure [29, 30], depending upon the composition symmetry. In most cases, however, one of the phases preferentially wets particles. In such a case, particles are included in the phase more wettable on a particle surface, which is the situation we consider here. Upon phase separation, wetting layers are quickly formed on particle surfaces [31] and then phase separation proceeds so that the phase more wettable for particles tends to include all the particles in it. This problem has been intensively studied both experimentally [16–20] and numerically [22–27].

One of the most drastic effects that affect the structure formation of particles in a binary mixture is capillary condensation [32–34], which produces a force so as to reduce the interfacial energy of the wetting layers bridging more than two particles. This effect also plays a crucial role in wet granular matter [35]. So far, this problem has been studied on the basis of 'energetic' interactions stemming from the wetting and interfacial energy. In our previous paper [36], however, we found a novel type of interaction of a purely dynamic origin, which can play an important role in the early stage of colloidal aggregation in a phase-separating binary mixture. This interaction is induced by the coupling of diffusion flux towards particles under the momentum conservation. Because of its intrinsically nonlocal nature, the interaction is non-additive. In this communication, we discuss the physical mechanism of this interaction in detail.

To study this problem of colloidal aggregation in a phase-separating fluid mixture, it is quite essential to take into account hydrodynamic interactions between particles [31]. Several numerical methods have been employed to study phase separation of binary fluids containing particles [22–27, 37]. On the basis of the 'fluid particle dynamics (FPD)' method [38, 39], we also developed a numerical method for describing dynamical couplings between particles, concentration and flow fields [36]. We note that our FPD method treats flow in a system in terms of a continuous field variable, which allows us to incorporate various continuous field variables (order parameters) into a host fluid without difficulty. Here we briefly explain our FPD method. Coarse-grained variables relevant for the physical description of phase-separation dynamics of a fluid mixture containing particles are particle position $\{\boldsymbol{r}_i\}$, concentration field ψ, and fluid velocity field $\boldsymbol{v}$. Index i stands for particle i. We describe fluid particle i using a hyperbolic tangent function as $\phi_i(\boldsymbol{r}) = [\tanh\{(a-|\boldsymbol{r}-\boldsymbol{r}_i|)/d\}+1]/2$, where a and d are the radius and interfacial width of a particle, respectively [38, 39]. We employ the following free energy functional for a binary mixture containing particles:

$$\mathcal{F}\{\psi,\phi\} = \int \mathrm{d}\boldsymbol{r}[f(\psi) - Wd\psi|\nabla\phi|^2 - \chi\Delta\psi^2\phi]. \quad (1)$$

The first term of the right-hand side (rhs) of equation (1) corresponds to the Ginzburg–Landau type mixing free energy of a binary mixture with $f(\psi) = \tau\psi^2/2 + u\psi^4/4 + K|\nabla\psi|^2/2$, where τ, u and K are constants (note that $\tau > 0$ before quench, $t < 0$). The second term stands for the wetting interaction between a binary mixture and a particle surface (represented as $|\nabla\phi|^2$ in our scheme). W represents the strength of this wetting interaction; here $W > 0$ means that the phase of $\psi > 0$ favours a particle surface. The third term is introduced such that the concentration field inside each particle is kept to $\psi \approx \bar{\psi}$. χ (>0) is the coupling constant and $\bar{\psi}$ is the average of ψ. Note that $\Delta\psi = \psi - \bar{\psi}$.

The time developments of ψ and $\boldsymbol{v}$ are described by

$$\frac{\partial\psi}{\partial t} = -\boldsymbol{v}\cdot\nabla\psi + L\nabla^2\mu, \quad (2)$$

$$\rho\frac{\partial\boldsymbol{v}}{\partial t} = \boldsymbol{G} - \psi\nabla\mu - \nabla p + \nabla\cdot\left[\eta\{\nabla\boldsymbol{v} + (\nabla\boldsymbol{v})^{\mathrm{T}}\}\right], \quad (3)$$

where μ is the chemical potential defined as $\mu = \delta\mathcal{F}/\delta\psi$. L and ρ are, respectively, the kinetic coefficient and the density, both of which are assumed to be independent of ψ. The characteristic length and time of phase separation are given as $\xi = (-K/\tau)^{1/2}$ and $t_\xi = \xi^2/L$, respectively. η is the space-dependent viscosity, which represents the particle distribution in our FPD scheme [38, 39]: $\eta(\boldsymbol{r}) = \bar{\eta} + \Delta\eta\sum_i \phi_i(\boldsymbol{r})$. The first term of the rhs of equation (3) is the force field stemming from particles: $\boldsymbol{G}(\boldsymbol{r}) = \sum_i \boldsymbol{G}_i\phi_i(\boldsymbol{r})$. Here $\boldsymbol{G}_i$ is the force acting on particle i, which is given by $\boldsymbol{G}_i = -(\partial/\partial\boldsymbol{r}_i)\sum_{j\neq i} V(|\boldsymbol{r}_i - \boldsymbol{r}_j|) - \kappa(\boldsymbol{r}_i - \boldsymbol{r}_i^f)$, where the second term of the rhs is introduced to fix the ith particle around the position $\boldsymbol{r}_i^f$ and κ is a spring constant. We employ the repulsive part of the Lennard-Jones potential as a direct interparticle interaction; $V(r) = 4\epsilon\{(2a/r)^{12} - (2a/r)^6 + 1/4\}$ for $r < 2^{7/6}a$ and $V(r) = 0$ for $r > 2^{7/6}a$. The second term of the rhs of equation (3) represents the force stemming from the osmotic pressure [40]. p is a part of pressure, which is imposed to satisfy the incompressibility condition $\nabla\cdot\boldsymbol{v} = 0$. The motion of particle i is given by the averaged velocity field inside the particle as [38, 39]

$$\frac{\mathrm{d}\boldsymbol{r}_i}{\mathrm{d}t} = \frac{\int \mathrm{d}\boldsymbol{r}'\boldsymbol{v}(\boldsymbol{r}')\phi_i(\boldsymbol{r}')}{\int \mathrm{d}\boldsymbol{r}'\phi_i(\boldsymbol{r}')}. \quad (4)$$

Hereafter we set the parameters as $u = 1$, $K = 1$ and $L = 1$. We solve the above kinetic equations with the explicit Euler scheme using the lattice spacing $\Delta x = 1$ and the time increment $\Delta t = 0.01$ in 2D and $\Delta t = 0.005$ in 3D. Equation (3) is solved by the marker and cell (MAC) method with a staggered lattice. To get rid of the inertia effect, we iterate the calculation of equation (3) to satisfy $|\rho\partial\boldsymbol{v}/\partial t| < 10^{-2}|\boldsymbol{G} - \psi\nabla\mu|$ (Stokes approximation). The viscosity parameters are set as $\bar{\eta} = 0.5$ and $\Delta\eta = 24.5$, which means that the viscosity ratio between the inner and outer parts of a particle is 50. The other parameters are set as $\xi = d = 1$, $\epsilon = 1$, $\chi = 2$, and $W = 8$ (except for two cases in figure 5(a)).

Figure 1(a) shows the behaviour of two free (unbound) particles ($\kappa = 0$) in a phase-separating mixture. At $t = 0$, we quench the system from the one-phase region ($\tau = 1$) to the coexistence region ($\tau = -1$). The volume fraction of the more wettable phase $\Psi = (\bar{\psi} + 1)/2$ is 0.10. The simulation is performed in 2D (128^2) and the particle radius and the initial separation are, respectively, $a = 8$ and $r_0 = |\boldsymbol{r}_{\mathrm{A}}(0) - \boldsymbol{r}_{\mathrm{B}}(0)| = 36$, where A and B stand for particles. Since the volume fraction of the more wettable minority phase is very low, the phase separation proceeds via a nucleation and growth (NG) mechanism. After the quench, the more wettable component nucleates on the particle surface to cover it ($t = 10t_\xi$): heterogeneous nucleation on particle surfaces. Then, the particles start to approach each other before their interfaces overlap ($t = 50t_\xi$). Eventually, they contact and share the wetting layer ($t = 200t_\xi$). To check whether this interaction is relevant only to the early stage, we quench the system while fixing the particle positions ($\kappa = 50$) and then (at $t = 5000t_\xi$) we release the particles by setting $\kappa = 0$. Figure 1(b) shows the behaviour of the two particles in a phase-separated mixture after the release. Although the interfaces are closer than in case (a), the particles do not move so much. Figure 1(c) shows

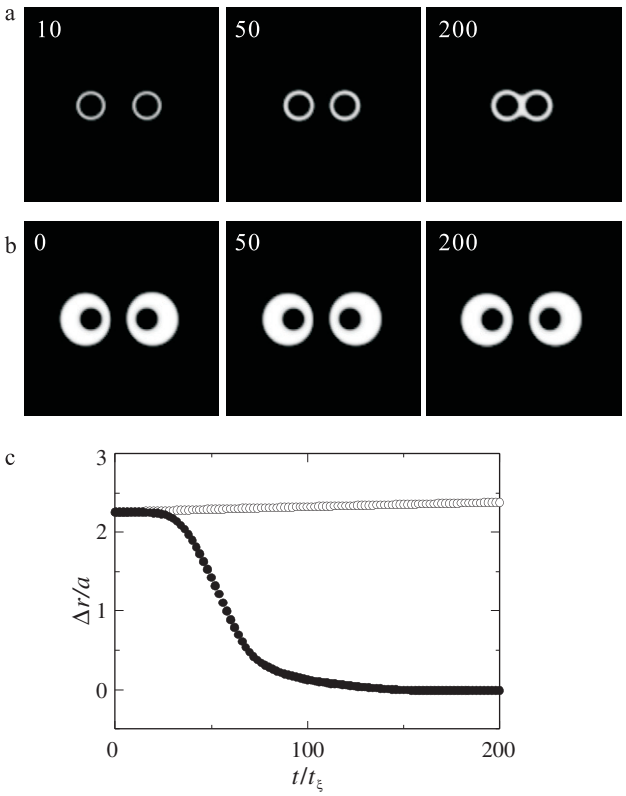

Figure 1. Behaviour of two particles in (a) phase-separating and (b) phase-separated binary mixtures. The brightness represents the compositional order parameter ψ. The brighter phase is more wettable for the particle surface. Numbers in the pictures represent t/t_ξ. (c) Temporal change in the separation between the two particles, $\Delta r = |\boldsymbol{r}_A - \boldsymbol{r}_B| - 2^{7/6}a$. ●: phase-separating mixture; ○: phase-separated mixture.

the temporal change in the separation between the two particles for cases (a) and (b). For a phase-separating mixture (case (a)), the particles attract each other until final contact. For a phase-separated mixture, on the other hand, there is no such strong attraction; the interparticle separation even slightly increases during the time since a particle tends to sit at the centre of the surrounding liquid droplet.

Next we show the temporal change in strength of the attractive force for different initial particle separations in figure 2 (3D). Here each particle is connected to a fixed point with a spring of $\kappa = 20$ such that the strength of the force can be measured as $F = \kappa|\boldsymbol{r} - \boldsymbol{r}^f|$. After the quench, the force grows quickly with time and then it starts to decrease gradually at a certain time. We can see that the force acting on the particles is stronger and the time at which the force has the maximum is shorter for the smaller interparticle separation. When the particle separation becomes smaller ($r_0/a < 4$), the force has a second peak. This second peak emerges when the wetting layers of the two particles overlap. Thus it is a consequence of the ordinary capillary interaction. During our simulation time, the wetting layers of the two particles do not contact each other for $r_0/a > 4$.

The dependence of the height of the first peak of the force on the particle separation is plotted in figure 3(a) (3D). The larger the interparticle separation, the weaker the force. The

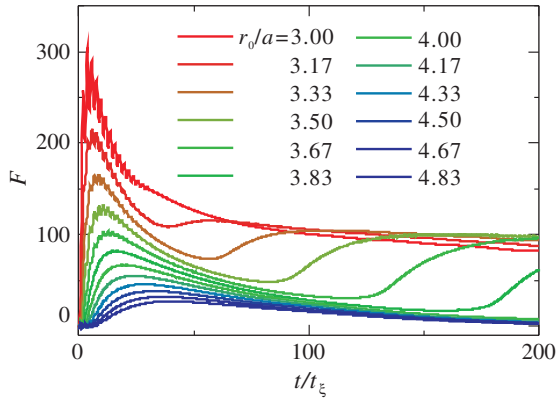

Figure 2. Dependence of the temporal change in the force acting on particles in a phase-separating mixture upon the particle separation. r_0/a is increasing from the top to the bottom. The simulations are performed in 3D (128^3). $\bar{\psi} = -0.8(\Psi = 0.10)$ and $a = 6$.

force strength approximately obeys $F \propto (r_0/a)^{-5}$. According to the two-scale factor universality [40], the interfacial tension is estimated as $\sigma \approx 0.1k_BT/\xi^2 \approx 4\ \mu\mathrm{N\,m^{-2}}$, for the interfacial width of $\xi = 10$ nm. For this case, $F = 100(\sigma\xi) \approx 4$ pN. Thus, this interaction can be much stronger and longer ranged than the van der Waals interaction and can have a significant influence on the aggregation behaviour.

Here we consider the physical origin of the interaction. As shown in figure 2, this interaction varies with time and the peaking time depends upon the interparticle separation. This indicates that the force is not produced by a potential. Tanaka previously proposed a mechanism of droplet coarsening in phase-separating fluid mixture due to a coupling between diffusion and hydrodynamic flow under momentum conservation [41, 42]. It predicts that such a dynamic coupling can induce attractive interactions between growing droplets. In the present system, particles behave as growing nuclei of phase separation, due to the surface wetting effects. Thus, we can apply this mechanism to particles immersed in a phase-separating fluid mixture.

Figure 4(a) shows the simulated diffusion flux $-L\nabla\mu$ at $t = 10t_\xi$. For an isolated particle, the diffusion flux and the resulting osmotic force $-\psi\nabla\mu$ are spherically symmetric. When two particles are placed nearby, on the other hand, the diffusion fluxes towards them are strongly coupled with each other. The more wettable component is depleted in between the particles and the resulting imbalance of the osmotic pressure pushes one particle towards another. As shown in figure 4(b), this induces the hydrodynamic flow, which transports one particle towards another. It is worth noting that this asymmetric diffusion flux leads to the non-concentric shape of droplets when the particle positions are fixed, as shown in figure 1(b) ($t/t_\xi = 0$).

To make a more quantitative estimate, we consider a single particle placed in a uniform concentration gradient. The situations that we consider here are the metastable state, where heterogeneous nucleation occurs selectively on the particle surface, and the one-phase region, where the prewetting layer is formed on the particle surface (see $\bar{\psi} < -1$ in

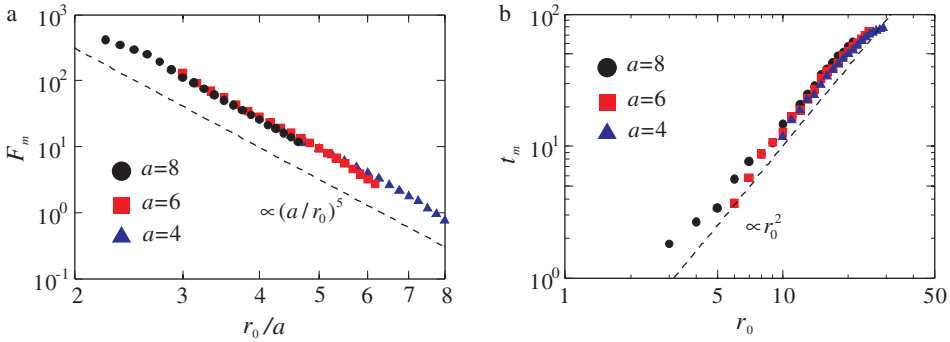

Figure 3. (a) Dependence of the maximum force strength on the particle separation, which is scaled as r_0/a. (b) Dependence of the time at which the attractive force is strongest on the particle separation. The simulations are performed in 3D (128^3). $\bar{\psi} = -0.8(\Psi = 0.10)$ and $W = 8$.

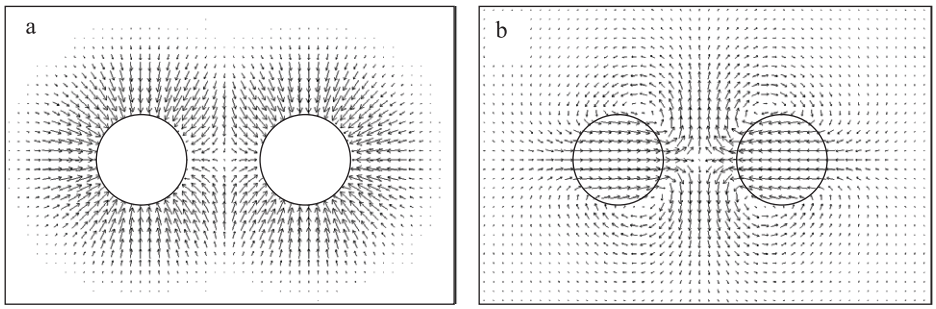

Figure 4. Simulated patterns of (a) diffusion flux $-L\nabla\mu$ and (b) flow field $\boldsymbol{v}$. The simulation is performed in 2D (128^2). $\bar{\psi} = -0.8(\Psi = 0.10)$ and $a = 8$.

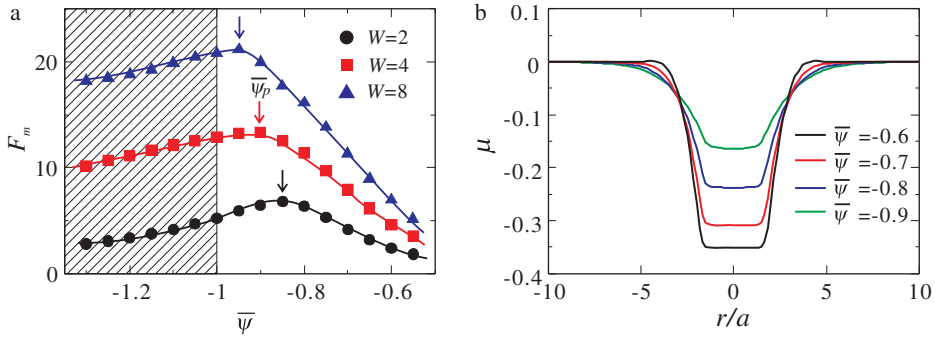

Figure 5. (a) The dependence of the maximum force strength $F_{\rm m}$ upon the averaged concentration $\bar{\psi}$ for different wettabilities W. The simulations are performed in 3D (128^3). $a = 6$ and $r_0 = 24$. The lines are guides to the eye. Even in the one-phase region (hatched area), this attractive interaction is observed. (b) The profiles of the chemical potential μ around a single particle at $t = 50t_\xi$. The particle radius is $a = 6$ and the wettability is $W = 8$. As $\bar{\psi}$ approaches the spinodal point ($\bar{\psi} = -1/\sqrt{3}$), the profile becomes sharper due to the nonlinear effects, which are ignored in our analytical treatment.

figure 5(a)). We do not consider the unstable state, where spinodal decomposition (SD) in the bulk creates randomly oriented diffusion fluxes, which overwhelm the directional flux towards the particle. Then, the concentration field, chemical potential, and pressure can be expressed as $X = X_0 + X_1(r) + X_2(r)\cos\theta$, where $X = \psi$, μ, and p, respectively, in a spherical coordinate system (r, θ, φ). We set the coordinate such that the particle is placed at $\boldsymbol{r} = 0$ and the concentration gradient is along $\theta = 0$. Then, the concentration gradient is produced by employing $\psi_2(r) = \alpha r$. Here we consider a case of weak gradient: $\alpha a \ll 1$. The flow field is also expressed as $\boldsymbol{v} = v_r(r)\cos\theta\hat{\boldsymbol{r}} + v_\theta(r)\sin\theta\hat{\boldsymbol{\theta}}$, where $\hat{\boldsymbol{r}}$ and $\hat{\boldsymbol{\theta}}$ are unit vectors of the spherical coordinate. Note that the φ-component of the flow should be zero from the symmetry. The hydrodynamic equations outside the particle, $-\psi\nabla\mu - \nabla p + \bar{\eta}\nabla^2\boldsymbol{v} = 0$ and $\nabla \cdot \boldsymbol{v} = 0$, impose a constraint on the linear order terms of $\cos\theta$ and $\sin\theta$, which yields the following relation [43]:

$$2(\psi_1'\mu_2 - \psi_2\mu_1') - \bar{\eta}(r^2 v_r'''' + 8r v_r''' + 8v_r'' - 8v_r'/r) = 0, \quad (5)$$

where the prime represents the derivative in terms of r. Here the incompressible condition, $v_\theta = -v_r - r v_r'/2$, is used.

Hereafter, we assume that the diffusion towards the particle surface is much stronger than that along the surface. Thus, we neglect the anisotropic part of the chemical potential and set $\mu_2 = 0$.

Immediately after the quench, the wetting layer is formed on the particle surface. Due to the conservation of ψ, the depletion zone of the more wettable component is formed around this wetting layer. The particle surface behaves as a sink, towards which the more wettable component is transported via diffusion. Here express the sink as $\beta\delta(|\boldsymbol{r}|-a)$, where β represents the strength of the sink and $\beta \sim W/\bar{\tau}$ in the first approximation. Near the binodal line, the conditions $\Delta\psi \ll 1$ and $|\bar{\psi}+1| \ll 1$ are satisfied, which allows us to neglect the nonlinear effects. Then, the concentration field around the particle approximately obeys the diffusion equation $\partial\Delta\psi/\partial t \approx D\nabla^2\Delta\psi$. Here $D = \bar{\tau}L$ is the diffusion coefficient, where $\bar{\tau} = \tau + 3u\bar{\psi}^2$. Its solution in the far field is given by $\Delta\psi \propto 4\pi a^2\beta \mathrm{e}^{-r^2/4Dt}/(4\pi Dt)^{3/2}$, where $4\pi a^2$ is the surface area of the particle. The chemical potential is approximately given as $\mu = \bar{\tau}\Delta\psi$. By substituting this into μ_1 in equation (5), we derive $v_r(r) = -\alpha\beta\bar{\tau}a^2\{2\mathrm{e}^{-r^2/4Dt}r\sqrt{Dt} + \sqrt{\pi}(r^2-2Dt)\,\mathrm{erf}(r/\sqrt{4Dt})\}/(2\sqrt{\pi}\bar{\eta}r^3)$. From the velocity of the particle surface $v_r(a)$, we obtain the particle drift velocity as $v \approx -\alpha\beta\bar{\tau}a^2/(3\sqrt{\pi}\bar{\eta}\sqrt{Dt})$.

Next we consider a pair of particles (A and B) separated by $r = r_0$ in a phase-separating fluid mixture. Here the concentration field formed around one particle acts as the concentration gradient for another. The concentration gradient at particle B is given by $\alpha \approx -\partial\Delta\psi/\partial r|_{r=r_0} = \beta a^2 r_0 \mathrm{e}^{-r_0^2/4Dt}/\{4\sqrt{\pi}(Dt)^{5/2}\}$ and the resulting approaching velocity is estimated as $v \approx -\beta^2\bar{\tau}a^4 r_0 \mathrm{e}^{-r_0^2/4Dt}/\{12\pi\bar{\eta}(Dt)^3\}$. This velocity becomes maximum at $t_\mathrm{m} = r_0^2/(2D)$ and the maximum velocity is $v_\mathrm{m} \approx -2\mathrm{e}^{-1/2}\beta^2\bar{\tau}a^4/(3\pi\bar{\eta}r_0^5)$. The maximum force acting on the particle pair is, thus, estimated as $F_\mathrm{m} = 6\pi\bar{\eta}a v_\mathrm{m} = -4\mathrm{e}^{-1/2}\beta^2\bar{\tau}(a/r_0)^5$. After $t = t_\mathrm{m}$, the force starts to becomes weaker with time due to the homogenization of the chemical potential. These relations, $F_\mathrm{m} \propto (r_0/a)^{-5}$ and $t_\mathrm{m} \propto r_0^2$, are consistent with the results of our numerical simulations shown in figures 3(a) and (b), respectively. When the particle separation is less than the particle size, i.e., for $(r_0 - 2a) < a$, a particle pair is approximately regarded as a pair of flat walls, which may lead to the weaker dependence of F_m on r_0. Such a tendency can be seen in figure 3(a).

Figure 5(a) shows the numerical results of the dependences of F_m on $\bar{\psi}$ for different wettabilities W. The force strength increases with increasing W, as expected. Each curve has a peak whose position $\bar{\psi}_\mathrm{p}$ shifts to lower $\bar{\psi}$ with an increase in W. Here we qualitatively explain this behaviour. Provided that $\beta \sim W/\bar{\tau}$, the force strength is proportional to $W^2/\bar{\tau}$. This means that the force strength monotonically increases towards the spinodal line, where $\bar{\tau}$ becomes zero. This increase simply reflects the decrease of the energy cost for producing the wetting layer with a decrease in $\bar{\tau}$. However, the above calculation cannot be used in the vicinity of the spinodal line, since there the nonlinear effects can no longer be neglected. In the mean-field approximation, the spinodal concentration is located at $|\bar{\psi}| < 1/\sqrt{3}(\approx 0.58)$. For the metastable region near the spinodal line, we confirmed by simulations that the concentration profile becomes sharper than that expected from the above simple diffusion equation due to the nonlinear effects, as shown in figure 5(b). Thus, the depletion zone does not reach the neighbouring particle. This qualitatively explains the weakening of the force. The competition between the weakening of the restoring force for concentration fluctuations and the nonlinear effects probably determines the position of the peak $\bar{\psi}_\mathrm{p}$. The nonlinear effects become dominant at lower $\bar{\psi}$ for larger W. This explains the shift of the peak position towards lower $\bar{\psi}$ with an increase in W.

It may be worth stressing that this attraction is observed even for mixtures of $\bar{\psi} < -1$, in which phase separation does not occur in the bulk (see figure 5(a)). Here a temperature quench thickens the prewetting layer on the particle surface, which accompanies the inward diffusion flux. This flux can induce attractive interactions, in the same manner as in phase separation.

In the unstable region, on the other hand, the diffusion fluxes far from the particle surface are not necessarily towards the particle surfaces for SD, since the system intrinsically becomes unstable. This prevents the formation of the well-developed depletion profile. Thus, when the particle separation is much larger than ξ, the wetting-induced depletion interaction no longer becomes effective, although it still remains [36].

In summary, we found a new type of attractive interaction between colloids in a phase-separating binary liquids. We demonstrated that this interaction is purely of a dynamic origin and a consequence of a dynamical coupling between the wetting-induced diffusion fluxes towards particles. This interaction may be confirmed experimentally by a direct measurement of the interparticle force with a laser tweezers. The temporal change in the force as in figure 2 may be observed. This interaction should quickly decay after the early stage of phase separation[1]. This characteristics may allow us to distinguish it from capillary force. Other types of numerical simulations, such as molecular dynamics [37] and lattice Boltzmann method [29], may also be useful for accessing the problem.

Finally, we note that this interaction should be generic to particles acting as diffusional sinks or sources. Thus, the mechanism may be relevant to a currently popular topic of particles self-propelled by diffusion phenomena [44]. Our study indicates that interparticle interactions can be induced not only by energetic or entropic origins, but also by a 'purely' dynamic origin. This may represent a new class of interparticle interaction that originates from a spatial coupling of a flux under the momentum conservation law.

This work was partially supported by a grant-in-aid from the Ministry of Education, Culture, Sports, Science and Technology, Japan.

References

[1] See, e.g. Poulin P, Stark H, Lubensky T C and Weitz D A 1997 *Science* **275** 1770

[1] Typically, it is about 10 times the characteristic diffusional time t_ξ. t_ξ is estimated as $t_\xi = 6\pi\eta\xi^3/k_\mathrm{B}T \approx 4.5$ μs for a mixture of $\xi = 10$ nm and $\bar{\eta} = 1$ mPa s at $T = 300$ K.

[2] Asakura S and Oosawa F 1955 *J. Chem. Phys.* **22** 1255
Poon W C K 2002 *J. Phys.: Condens. Matter* **14** R859
[3] Balazs A C, Emrick T and Russell T P 2006 *Science* **314** 1007
[4] Cahn J W 1985 *J. Chem. Phys.* **66** 3667
[5] de Gennes P G 1985 *Rev. Mod. Phys.* **57** 827
[6] Beysens D and Estève D 1985 *Phys. Rev. Lett.* **54** 2123
[7] Beysens D and Narayanan T 1999 *J. Stat. Phys.* **95** 997
[8] Löwen H 1995 *Phys. Rev. Lett.* **74** 1028
[9] Netz R R 1996 *Phys. Rev. Lett.* **76** 3646
[10] Law B M, Petit J M and Beysens D 1998 *Phys. Rev.* E **57** 5782
[11] Petit J M, Law B M and Beysens D 1998 *J. Colloid Interface Sci.* **202** 441
[12] Benhamou M, Ridouane H, Hachem E K, Derouiche A and Rahmoune M 2005 *J. Chem. Phys.* **122** 244913
[13] Schlesener F, Hanke A and Dietrich S 2003 *J. Stat. Phys.* **110** 981
[14] Fisher M E and de Gennes P G 1978 *C. R. Acad. Sci. Paris* B **287** 207
[15] Puri S 2005 *J. Phys.: Condens. Matter* **17** R101
[16] Tanaka H 2001 *J. Phys.: Condens. Matter* **13** 4637
[17] Tanaka H, Lovinger A J and Davis D D 1994 *Phys. Rev. Lett.* **72** 2581
[18] Karim A, Douglas J F, Nisato G, Liu D W and Amis E J 1999 *Macromolecules* **32** 5917
[19] Lee B P, Douglas J F and Glotzer S C 1999 *Phys. Rev.* E **60** 5812
[20] Chung H J, Taubert A, Deshmunkh R D and Composto R J 2004 *Europhys. Lett.* **68** 219
[21] Ma Y Q 2000 *Phys. Rev.* E **62** 8207
[22] Qiu F, Peng G, Ginzburg V V, Balaz A C, Chen H Y and Jasnow D 2001 *J. Chem. Phys.* **115** 3779
[23] Suppa D, Kuksenok O, Balaz A C and Yeomans J M 2002 *J. Chem. Phys.* **116** 6305
[24] Verberg R, Yeomans J M and Balazs A C 2005 *J. Chem. Phys.* **123** 224706
[25] Laradji M and MacNevin G 2003 *J. Chem. Phys.* **119** 2275
[26] Tang Y L and Ma Y Q 2002 *J. Chem. Phys.* **116** 7719
[27] Laradji M and Hore M J A 2004 *J. Chem. Phys.* **121** 10641
[28] Binks B P and Clint J H 2002 *Langmuir* **18** 1270
[29] Stratford K, Adhikari R, Pagonabarraga I, Desplat J C and Cates M E 2005 *Science* **309** 2198
[30] Herzig E M, White K A, Schofield A B, Poon W C K and Clegg P S 2007 *Nat. Mater.* **6** 966
[31] Tanaka H and Araki T 2000 *Europhys. Lett.* **51** 154
[32] Bauer C, Bieker T and Dietrich S 2000 *Phys. Rev.* E **62** 5324
[33] Andrienko D, Patrício P and Vinogradova O I 2004 *J. Chem. Phys.* **121** 4414
[34] Evans R, Marconi U M B and Tarazona P 1986 *J. Chem. Phys.* **84** 2376
[35] Herminghaus S 2005 *Adv. Phys.* **54** 221
[36] Araki T and Tanaka H 2006 *Phys. Rev.* E **73** 061506
[37] Chakrabarti J, Chakrabarti S and Löwen H 2006 *J. Phys.: Condens. Matter* **18** L81
[38] Tanaka H and Araki T 2000 *Phys. Rev. Lett.* **85** 1338
[39] Tanaka H and Araki T 2006 *Chem. Eng. Sci.* **61** 2108
[40] Onuki A 2002 *Phase Transition Dynamics* (Cambridge: Cambridge University Press)
[41] Tanaka H 1996 *J. Chem. Phys.* **105** 10099
[42] Tanaka H 1997 *J. Chem. Phys.* **109** 3734
[43] Fujitani Y 2006 *J. Phys. Soc. Japan* **75** 013401
[44] see, e.g. Thakur S, Sunil Kumar P B, Madhusudana N V and Pullarkat P A 2006 *Phys. Rev. Lett.* **97** 115701 and references therein